Inorganic Chemistry
Article

Inorg. Chem. **2010**, *49*, 7685–7691 **7685**
DOI: 10.1021/ic100212q

Porous Coordination Polymers of Transition Metal Sulfides with PtS Topology Built on a Semirigid Tetrahedral Linker

Jun Zhang, Yun-Shan Xue, Li-Li Liang, Shi-Bin Ren, Yi-Zhi Li, Hong-Bin Du,* and Xiao-Zeng You

State Key Laboratory of Coordination Chemistry, School of Chemistry and Chemical Engineering, Nanjing University, Nanjing, 210093, China

Received February 3, 2010

Four novel porous metal sulfide coordination polymers, $[M(tpom)S_x(SH)_y]\cdot z(H_2O)$ (metal-sulfide frameworks, denoted MSF-*n*, *n* = 1, Cd; 2, Mn; 3, Fe; 4, Co; *x* = 0, *y* = 2 for 1, 2, and 4 and *x* = 0.54, *y* = 1.46 for 3), were solvothermally prepared by using a quadridentate linker, tetrakis(4-pyridyloxymethylene)methane (tpom), in the presence of organic sulfur compound under an acidic conditions. MSF-*n* (*n* = 1−4) is isostructural and built upon the tetrahedral tpom linker and square planar $MS_x(SH)_y$ unit, which form a binodal 4,4-connected porous framework with a 2-fold interpenetrated 4^28^4-**pts** net. With rectangular pore channels of about 5 × 6 $Å^2$ (interatomic distances between the nearest protruding H atoms across) running along both the crystallographic *a* and *b* directions, MSF-*n* possesses permanent porosity with a BET surface area of 575, 622, 617, and 767 m^2/g for MSF-1, -2, -3, and -4, respectively, as estimated from N_2 adsorption measurements. MSF-*n* (*n* = 1−4) has hydrogen storage capacities of 1.03, 1.37, 1.29, and 1.58 wt % at 77 K and 1 atm, respectively, each corresponding to 2.0 H_2 molecules per unit cell. In addition, MSF-*n* (*n* = 1−4) can adsorb 24.1, 25.0, 21.6, and 24.1 wt % of carbon dioxide and 6.0, 6.1, 5.6, and 6.4 wt % of methane, respectively, at room temperature and 20 atm.

Introduction

Porous coordination polymers have been subjects of intense research because of their intriguing structures and potential applications in adsorbents, molecular sieving, catalysis, luminescence, etc.[1] These materials are usually three-dimensional (3D) open frameworks constructed from the combination of metal ions or clusters with multidentate organic ligands through more or less covalent metal−ligand bonding. The availability of various organic ligands of certain geometry and functionality has allowed the rational synthesis of porous coordination polymers with specific structure and properties. Therefore, considerable current research efforts have been devoted to the preparation of new organic ligands and their use in the assembly of new coordination polymers.

Among various ligands reported so far in the construction of coordination polymers are dominant nitrogen- and oxygen-donor bridging linkers, such as carboxylic acids, pyridine derivatives, etc.[2] We are interested in the design and synthesis of porous coordination polymers of metal chalcogenides with multidentate ligands. These materials may possess structures and properties which differ from their N- and O-bridging counterparts. They may resemble previously reported open-framework metal chalcogenides such as CdS and GeS_2, which are capable of integrating porosity with electrical or optical properties and hold promise for applications beyond those of traditional insulating oxides, e.g., as solid electrolytes, semiconductor electrodes, sensors, and photocatalysis.[3] On the other hand, coordination compounds of the transition metals bearing the ligands SH^-, S^{2-}, S_2^{2-}, and H_2S potentially could serve as models for biological systems.[4] We used a semirigid tridentate (2,4,6-trimethylbenzene-1,3,5-triyl)trimethanethiol (tbms) in the presence of a tetradentate tetrakis-(4-pyridyloxymethylene)methane (tpom) as a coligand to react with transition metal ions in a solvothermal system (Scheme 1) and serendipitously obtained four isostructural coordination polymers $[M(tpom)S_x(SH)_y]\cdot z(H_2O)$ (M = Cd, Mn, Fe, Co), denoted MSF-*n* (*n* = 1, 2, 3, and 4, metal-sulfide-framework), respectively. It is interesting that

*To whom correspondence should be addressed. Tel.: 86-25-83686581. Fax: 86-25-83314502. E-mail: hbdu@nju.edu.cn.

(1) (a) Morris, R. E.; Wheatley, P. S. *Angew. Chem., Int. Ed.* **2008**, *47*, 4966. (b) Dinc, M.; Long, J. R. *Angew. Chem., Int. Ed.* **2008**, *47*, 6766. (c) Allendorf, M. D.; Bauer, C. A.; Bhakta, R. K.; Houk, R. J. T. *Chem. Soc. Rev.* **2009**, *38*, 1330. (d) Czaja, A. U.; Trukhan, N.; Muller, U. *Chem. Soc. Rev.* **2009**, *38*, 1284.

(2) (a) Janiak, C. *Dalton Trans.* **2003**, 2781. (b) Long, J. R.; Yaghi, O. M. *Chem. Soc. Rev.* **2009**, *38*, 1213 special issues. (c) Yaghi, O. M.; O'Keeffe, M.; Ockwig, N. W.; Chae, H. K.; Eddaoudi, M.; Kim, J. *Nature* **2003**, *423*, 705. (d) Banerjee, R.; Phan, A.; Wang, B.; Knobler, C.; Furukawa, H.; O'Keeffe, M.; Yaghi, O. M. *Science* **2008**, *319*, 939.

(3) (a) Husing, N. *Angew. Chem., Int. Ed.* **2008**, *47*, 1992. (b) Feng, P.; Bu, X.; Zheng, N. *Acc. Chem. Res.* **2005**, *38*, 293. (c) Vittal, J. J.; Ng, M. T. *Acc. Chem. Res.* **2006**, *39*, 869. (d) Wachhold, M.; Rangan, K. K.; Lei, M.; Thorpe, M. F.; Billinge, S. J. L.; Petkov, V.; Heising, J.; Kanatzidis, M. G. *J. Solid State Chem.* **2000**, *152*, 21.

(4) (a) Kovacs, J. A.; Brines, L. M. *Acc. Chem. Res.* **2007**, *40*, 501. (b) Henderson, R. A. *Chem. Rev.* **2005**, *105*, 2365. (c) Lee, S. C.; Holm, R. H. *Chem. Rev.* **2004**, *104*, 1135.

Published on Web 07/27/2010

Scheme 1. Synthesis of Complexes MSF-*n*

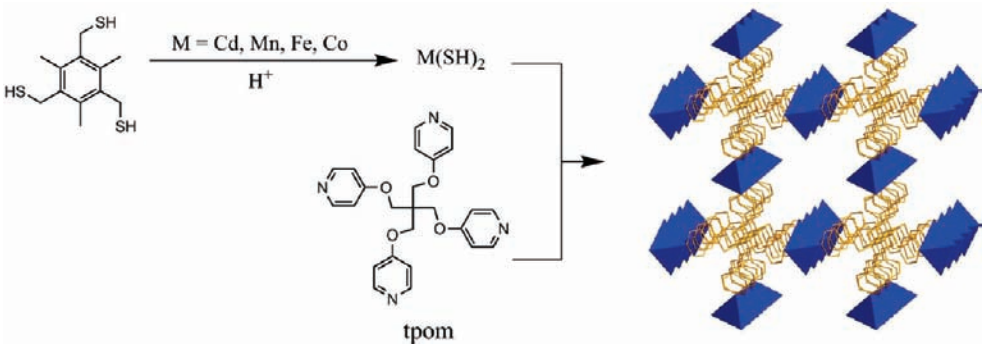

the resulting materials do not consist of tbms, instead composed of metal hydrosulfide and tpom as revealed by X-ray single crystal structure analyses. We herein report their syntheses, structure analyses, and adsorption properties.

Experimental Details

Materials. All commercially available chemicals are of reagent grade and were used as received without further purification. The ligand tpom was synthesized according to the literature[5] and the ligand tbms according to the literature.[6]

Physical Measurements. Elemental analyses of C, H, and N were performed on a Elementar Vario MICRO Elemental Analyzer at the Analysis Center of Nanjing University. Fourier transformed Infrared (FT-IR) spectra were obtained on a Bruker Vector 22 FT-IR spectrophotometer by using KBr pellets. Thermogravimetrical and differential thermal analyses (TG-DTA) were performed in a N_2 atmosphere (a flow rate of 100 mL min^{-1}) on a simultaneous SDT 2960 thermal analyzer from 35 °C up to 750 °C, with a heating rate of 10 °C/min. X-ray powder diffraction (XRPD) data were collected on a Bruker D8 Advance instrument using Cu Kα radiation (λ = 1.54056 Å) at room temperature. The adsorption isotherms of nitrogen and hydrogen were measured at 77 K by using Micromeritics ASAP 2020 M+C volumetric adsorption equipment. The samples were pretreated at 373 K under a 50 μm Hg vacuum for about 10 h prior to the measurement of the isotherms. High-pressure carbon dioxide and methane sorption isotherm measurements were carried out on a Hiden Isochema IGA 100 high-pressure instrument at room temperature. Prior the measurements, approximately 100 mg of samples were placed in a stainless-steel sample holder and degassed at 373 K under a 10 mbar vacuum for about 5 h. Mossbauer spectroscopy was obtained on a German Wissel Mossbauer spectrometer.

Preparation of $[Cd(tpom)(SH)_2]\cdot 4H_2O$ (MSF-1). To the solution of tbms (0.024 g, 0.093 mmol) in 1.5 mL of N,N-dimethylformamide (DMF) was added a solution of $Cd(NO_3)_2\cdot 4H_2O$ (0.031 g, 0.10 mmol) in DMF (1.5 mL) to give a white solid. Aqueous HCl (1:1 volume) was added dropwise to the mixture until the solid disappeared, where the pH was about 5. To the above solution was added the solution of tpom (0.022 g, 0.049 mmol) in DMF (2 mL). A white precipitate appeared and disappeared after adding a drop of aqueous HCl (1:1; pH ~ 5). The mixture was transferred into a vial, which was then sealed and heated at 100 °C for 3 days. The vial was then allowed to cool down to room temperature. Colorless octahedral crystals (0.031 g) were obtained by filtration and washed with DMF and acetonitrile three times each, respectively. Yield: 91.2% (based on tpom). Anal. Calcd for $C_{25}H_{34}CdN_4O_8S_2$: C, 43.20; H, 4.93; N, 8.06%. Found: C, 43.49; H, 4.81; N, 8.28%. FT-IR (KBr, cm^{-1} (rel. int.)): 3448 (5, b), 3067 (6), 2947 (6), 2887 (5), 2500 (3,ν_{S-H}), 1603 (100), 1567 (64), 1506 (75), 1460 (53), 1430 (34), 1288 (86), 1211 (95), 1020 (71), 867 (28), 844 (50), 818 (54), 735 (28), 698 (11), 532 (28).

Preparation of $[Mn(tpom)(SH)_2]\cdot 2H_2O$ (MSF-2). Orange octahedral crystals of MSF-2 were obtained by following the same procedure of MSF-1 with the replacement of $Cd(NO_3)_2\cdot 4H_2O$ with $MnCl_2\cdot 4H_2O$, and crystallization at 120 °C. Yield: 75.0% (based on tpom). Anal. Calcd for $C_{25}H_{30}MnN_4O_6S_2$: C, 49.91; H, 5.03; N, 9.31%. Found: C, 49.99; H, 5.07; N, 9.23%. FT-IR (KBr, cm^{-1} (rel. int.)): 3409 (4, b), 3058 (5), 2950 (4), 2884 (3), 2492 w (2, ν_{S-H}), 1603 (100), 1568 (50), 1504 (63), 1466 (38), 1431 (23), 1288 (76), 1211 (86), 1020 (60), 872 (19), 846 (38), 816 (42), 735 (14), 534 (21).

Preparation of $[Fe(II)_{0.46}Fe(III)_{0.54}(tpom)S_{0.54}(SH)_{1.46}]\cdot 2H_2O$ (MSF-3). Orange octahedral crystals of MSF-3 were obtained by following the same procedure of MSF-1 with the replacement of $Cd(NO_3)_2\cdot 4H_2O$ with $FeCl_2\cdot 4H_2O$. Yield 73.33% (based on tpom). Anal. Calcd for $C_{25}H_{29.46}FeN_4O_6S_2$: C, 49.88; H, 4.93; N, 9.31%. Found: C, 49.91; H, 4.87; N, 9.41%. FT-IR (KBr, cm^{-1} (rel. int.)): 3406 (7, b), 3067 (9), 2947 (4), 2887 (4), 2493 (2, ν_{S-H}), 1930 (3), 1603 (100), 1567 (61), 1506 (81), 1460 (60), 1426 (30), 1286 (93), 1207 (97), 1020 (71), 873 (27), 846 (45), 820 (53), 740 (9), 533 (26).

Preparation of $[Co(tpom)(SH)_2]\cdot 2H_2O$ (MSF-4). Violet red octahedral crystals of MSF-4 were obtained by following the same procedure of MSF-1 with the replacement of $Cd(NO_3)_2\cdot 4H_2O$ with $Co(NO_3)_2\cdot 6H_2O$. Yield: 93.5% (based on tpom). Anal. Calcd for $C_{25}H_{30}CoN_4O_6S_2$: C, 49.58; H, 4.99; N, 9.25%. Found: C, 49.61; H, 4.86; N, 9.37%. FT-IR (KBr, cm^{-1} (rel. int.)): 3421 (4, b), 3061 (5), 2941 (4), 2881 (3), 2494 (2, ν_{S-H}), 1926 (1), 1608 (100), 1568 (51), 1504 (63), 1463 (38), 1433 (23), 1288 (79), 1211 (88), 1021 (20), 873 (19), 846 (38), 820 (42), 735 (14), 533 (20).

X-Ray Diffraction Determinations. The data collections for single crystal X-ray diffraction for MSF-1 to MSF-4 were carried out on a Bruker Smart APEX II CCD diffractometer at 291 K, using graphite-monochromated Mo Kα radiation (λ = 0.71073 Å). Data reductions and absorption corrections were performed using the SAINT and SADABS programs,[7] respectively. The structures were solved by direct methods using the SHELXS-97 program[8] and refined with full-matrix least-squares on F^2 using the SHELXL-97 program.[9] All non-hydrogen atoms were refined anisotropically, and all of the hydrogen atoms were set in geometrically calculated positions and refined using a riding model. The water molecules in the channels of the structure are disordered. We employed PLATON/SQUEEZE

(5) Metrangolo, P.; Meyer, F.; Pilati, T.; Proserpio, D. M.; Resnati, G. *Chem.—Eur. J.* **2007**, *13*, 5765.
(6) Aversa, M. C.; Barattucci, A.; Bonaccorsi, P.; Faggi, C.; Papalia, T. *J. Org. Chem.* **2007**, *72*, 4486.
(7) *SMART*; *SADABS*; Bruker AXS Inc.: Madison, Wisconsin.
(8) Sheldrick, G. M. *SHELXS-97*; University of Göttingen: Göttingen, Germany, 1997.
(9) Sheldrick, G. M. *SHELXS-97*; University of Göttingen: Göttingen, Germany, 1997.

Table 1. Crystallographic Data for MSF-1 to -4

compound	MSF-1	MSF-2	MSF-3	MSF-4
chemical formula	$C_{25}H_{34}CdN_4O_8S_2$	$C_{25}H_{30}MnN_4O_6S_2$	$C_{25}H_{29.46}FeN_4O_6S_2$	$C_{25}H_{30}CoN_4O_6S_2$
fw	695.08	601.59	601.96	605.58
cryst syst	tetragonal	tetragonal	tetragonal	tetragonal
space group	$P4(2)/n$	$P4(2)/n$	$P4(2)/n$	$P4(2)/n$
T (K)	291(2)	291(2)	291(2)	291(2)
wavelength (Å)	0.71073	0.71073	0.71073	0.71073
a (Å)	12.2731(8)	12.1750(7)	12.1470(4)	12.0790(9)
c (Å)	25.135(3)	24.924(3)	24.744(2)	24.539(4)
V (Å^3)	3786.1(6)	3694.6(5)	3651.0(3)	3580.3(6)
Z	4	4	4	4
D_{calcd} (g cm^{-3})	1.219	1.082	1.095	1.123
abs coeff (mm^{-1})	0.728	0.505	0.562	0.632
F(000)	1424	1252	1253.8	1260
cryst size (mm^3)	0.20 × 0.18 × 0.18	0.30 × 0.24 × 0.22	0.28 × 0.22 × 0.20	0.28 × 0.24 × 0.22
reflns collected	20121	18427	18322	19396
independent reflns/R_{int}	3724/0.0653	3252/0.0667	3228/0.0730	3524/0.0779
reflns observed ($I > 2\sigma(I)$)	2390	1933	2027	2189
GOF on F^2	1.031	1.073	1.068	1.035
R_1, wR_2 ($I > 2\sigma(I)$)[a]	0.0544/0.1223	0.0540/0.1509	0.0521/0.1441	0.0490/0.1049
R_1, wR_2 (all data)[a]	0.0843/0.1284	0.0941/0.1747	0.0852/0.1722	0.0830/0.1151
largest diff. peak and hole (e Å^{-3})	0.485/−0.984	0.477/−0.541	0.292/-0.276	0.219/−0.417

[a] $R_1 = \sum\|F_o| - |F_c\|/\sum|F_o|$, $wR_2 = [\sum w(F_o^2 - F_c^2)^2/\sum w(F_o^2)^2]^{1/2}$.

Table 2. Selected Interatomic Distances (Å) and Angles (deg) for MSF-1 to -4[a]

		MSF-1			
Cd1−N1	2.397(4)	Cd1−N2^{i}	2.393(4)	Cd1−S1	2.576(1)
N1−Cd1−N1^{iii}	86.8 (2)	N1−Cd1−S1	90.2(1)	N1^{iii}−Cd1−S1	88.4 (1)
N2^{i}−Cd1−N1	178.3 (1)	N2^{ii}−Cd1−N1	91.9(1)	N2^{i}−Cd1−N2^{ii}	89.5(2)
N2^{i}−Cd1−S1	90.8(1)	N2^{ii}−Cd1−S1	90.6(1)	S1−Cd1−S1^{iii}	178.12(6)
		MSF-2			
Mn1−N1	2.319(3)	Mn1−N2^{i}	2.317(3)	Mn1−S1	2.5018(9)
N1^{iii}−Mn1−N1	87.1(2)	N1−Mn1−S1	90.82(8)	N1^{iii}−Mn1−S1	88.77(8)
N2^{ii}−Mn1−N1	178.7(1)	N2^{i}−Mn1−N1	92.1(1)	N2^{i}−Mn1−N2^{ii}	88.6(2)
N2^{i}−Mn1−S1^{iii}	90.26(8)	N2^{i}−Mn1−S1	90.15(8)	S1^{iii}−Mn1−S1	179.43(6)
		MSF-3			
Fe1−N1	2.252(3)	Fe1−N2^{ii}	2.274(3)	Fe1−S1	2.4500(9)
N1−Fe1−N1^{i}	88.4(1)	N1−Fe1−S1	88.75(8)	N1−Fe1−S1^{i}	89.79(8)
N2^{ii} −Fe1−N1	178.9(1)	N2^{ii}−Fe1−N1^{i}	91.9(1)	N2^{ii}−Fe1−N2^{iii}	87.8(2)
N2^{ii}−Fe1−S1^{i}	91.32(7)	N2^{iii}−Fe1−S1^{i}	90.15(7)	S1^{i}−Fe1−S1	177.96(5)
		MSF-4			
Co1−N1	2.193(3)	Co1−N2^{ii}	2.223(3)	Co1−S1	2.4505(7)
N1^{i}−Co1−N1	87.7(1)	N1−Co1−S1	89.10(7)	N1^{i}−Co1−S1	89.76(7)
N2^{ii}−Co1−N1	179.4(1)	N2^{ii}−Co1−N1^{i}	92.0(1)	N2^{ii}−Co1−N2^{iii}	88.3(1)
N2^{ii}−Co1−S1	90.42(7)	N2^{iii}−Co1−S1	90.72(7)	S1−Co1−S1^{i}	178.41(5)

[a] Symmetry transformations. For MSF-1: (i) $1-y, -0.5+x, -0.5+z$; (ii) $-0.5+y, 1-x, -0.5+z$; (iii) $0.5-x, 0.5-y, z$. For MSF-2: (i) $0.5+y, 1-x, -0.5+z$; (ii) $2-y, 0.5+x, -0.5+z$; (iii) $2.5-x, 0.5-y, z$. For MSF-3: (i) $0.5-x, 0.5-y, z$; (ii) $-0.5+y, -x, -0.5+z$; (iii) $1-y, 0.5+x, -0.5+z$. For MSF-4: (i) $0.5-x, 0.5-y, z$; (ii) $-0.5+y, -x, -0.5+z$; (iii) $1-y, 0.5+x, -0.5+z$.

to calculate the diffraction contribution of the solvent molecules and, thereby, located the solvent molecules in the difference Fourier map and refined their atomic parameters.[10] Mossbauer spectroscopy reveals that 53.8% of the metal in MSF-3 is Fe(III) and 46.2% is Fe(II) (Figure S1, Supporting Information), which were used in the final refinement of MSF-3. Details of the crystal parameters, data collection, and refinement results are summarized in Table 1. Selected interatomic distances and angles with their estimated standard deviations are given in Table 2. Further details can be obtained from the Supporting Information. CCDC reference numbers are 763094−763097.

Results and Discussion

Synthesis. MSF-n (n = 1−4) was prepared solvothermally in the presence of thiol ligand tbms and pyridine ligand tpom. X-ray single crystal analyses showed that MSF-n's are coordination polymers of metal sulfides constituting metal hydrosulfide and the tpom ligand. The presence of the S−H groups is supported by the weak vibration peak around 2500 cm^{-1} in the FT-IR spectrum

(10) Spek, A. L. *J. Appl. Crystallogr.* **2003**, *36*, 7–13. Spek, A. L. *PLATON*; Utrecht University: Utrecht, The Netherlands, 2006, available via http://www.cryst.chem.uu.nl/platon (for Unix) and http://www.chem.gla.ac.uk/Blouis/software/platon/ (for MS Windows).

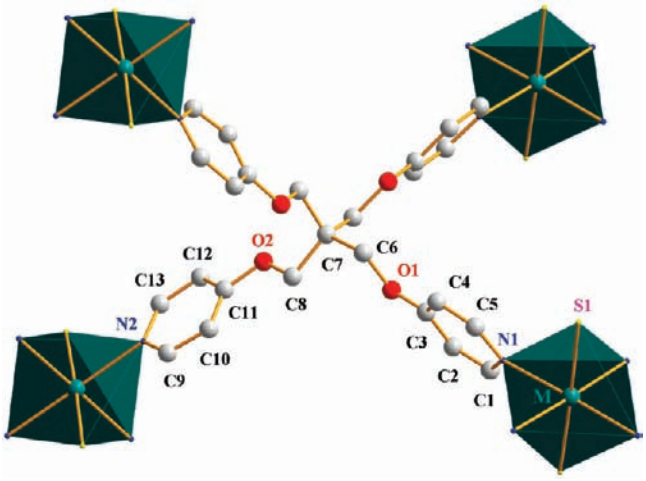

Figure 1. Perspective drawing showing the building units in MSF-*n* (M = Cd, Mn, Fe, Co). The H atoms are omitted for clarity.

of each compound. Therefore, we postulated that ligand tbms serves as a sulfur source as a result of its hydrolysis under hydrothermal conditions. The release of the −SH group from the thiols has been known to lead to the formation of metal sulfide nanoparticles or SH-bridged complexes.[11] Other organic sulfur compounds, e.g., naphthalene-1,5-dithiol and (2,4,6-trimethylbenzene-1,3,5-triyl)tris(methylene)tris(ethylsulfane), can also be used for the formation of MSF-*n* (n = 1−4), while sodium hydrosulfide results in the precipitation of inorganic metal sulfides. Besides Cd, Mn, Fe, and Co, Cu also forms an isostructural compound under similar conditions as evidenced by preliminary X-ray single crystal structure analysis. Attempts to prepare analogues of Zn and Ni have so far met with failures. MSF-*n* (n = 1−4) is insoluble in common solvents such as methanol, ethanol, acetone, acetonitrile, ether, DMF, and water and are stable in the air. The crystals are still transparent after several months. The phase purity for each product was confirmed by elemental analyses and X-ray powder diffraction.

Crystal Structure Descriptions. X-ray single crystal diffraction analyses revealed that MSF-*n* (n = 1−4) is isostructural, and all crystallize in the centrosymmetric tetragonal space group $P4_2/n$, which is associated with the point group C_{4h}. The compounds are built from a metal disulfide unit and the flexible ligand tpom. The asymmetric unit of each compound consists of a half metal ion, one −S, a half ligand tpom, and two guest water molecules for MSF-1 and one guest water molecule for MSF-2 to -4 (Figure S2, Supporting Information). As shown in Figure 1, the M center adopts a slightly distorted octahedral coordination geometry, in which two axial positions are occupied by charge-balancing terminal −SH and −S (MSF-3) groups, while four equatorial positions are coordinated by nitrogen atoms from four different neutral tpom ligands. The M−N interatomic distances range 2.393(4)−2.397(4), 2.317(3)−2.319(3), 2.252(3)−2.274(3), and 2.193(3)−2.223(3) Å for MSF-1 (Cd), MSF-2 (Mn), MSF-3 (Fe), and MSF-4 (Co), respectively, consistent with those reported for other respective metal−pyridine complexes.[12] The M−S bonds are within normal ranges,[13] with interatomic distances of 2.576(1) (Cd, MSF-1), 2.5018(9) (Mn, MSF-2), 2.4500(9) (Fe, MSF-3), and 2.4505(7) Å (Co, MSF-4), respectively. The quadridentate linker tpom, on the other hand, adopts a distorted tetrahedral geometry (with exact C_2 symmetry), coordinating to four metal ions. It has tetrahedron edge lengths of *ca.* 8.939(7)−11.133(5) (MSF-1), 8.973(5)−11.141(5) (MSF-2), 9.026(5)−11.154(4) (MSF-3), and 9.024(4)−11.126(4) Å (MSF-4), respectively, as measured between the terminal N atoms. The angles around the tetrahedron center carbon atom are within the ranges of 88.79(5)−120.78(5), 88.70(4)−120.74(4), 89.23(4)−120.59(3), and 89.33(3)−120.24(3)° for MSF-1 (Cd), MSF-2 (Mn), MSF-3 (Fe), and MSF-4 (Co), respectively.

The frameworks of MSF-*n* (n = 1−4) are constructed from a 4-connecting MS_2 unit and a quadridentate linker, tpom. Each quadridentate tpom tetrahedrally coordinates via its N-donor atoms to four MS_2 units, while each MS_2 unit connects, in a square planar geometry, with four tpom ligands. This gives rise to a binodal 4,4-connecting 3D framework with 4^28^4−**pts** (PtS) topology (Figure 2). The MS_2 square planar node has a point symbol of 4^28^4 and vertex symbol of 4.4.8(2).8(2).8(8).8(8), while the tpom tetrahedral node has the same point symbol of 4^28^4 but a different vertex symbol of 4.4.8(7).8(7).8(7).8(7).[14] The **pts** net with large cavities interpenetrates another identical one, leading to a 2-fold interpenetration network of MSF-*n* (n = 1−4). The interpenetration can be regarded as space filling to stabilize the framework,[15] leading to the elimination of parts of the free space in MSF-*n* (n = 1−4). The remaining free voids are filled with guest water molecules. The topologically rectangular 1D channels run along both the crystallographic *a* and *b* directions with sizes of ca. 5.9 × 6.1 (MSF-1), 5.5 × 6.6 (MSF-2), 5.0 × 5.5 (MSF-3), and 5.6 × 6.8 (MSF-4) Å^2, respectively, measured as interatomic distances between the nearest protruding H atoms across (Figure 3). Calculations using PLATON[10] based on the crystal structures show that the total solvent-accessible volume is about 1522, 1471, 1453, and 1407 Å^3 per unit cell, comprising 40.2, 39.8, 39.8, and 39.3% of the total crystal volume for MSF-1 to -4, respectively. The relatively large solvent-accessible voids together with the terminal M−S or M−SH groups in MSF-*n* could render them potentially useful as adsorbents or catalysts.

(11) (a) Mao, W.; Guo, J.; Yang, W.; Wang, C.; He, J.; Chen, J. *Nanotechnology* **2007**, *18*, 485611. (b) Rogach, A. L. *Mater. Sci. Eng.* **2000**, *B69−70*, 435. (b) Ahmad, T.; Rüffer, T.; Lang, H.; Isab, A. A.; Ahmad, S. *Inorg. Chim. Acta* **2009**, *362*, 2609. (c) Han, L.; Zhao, W.; Zhou, Y.; Li, X.; Pan, J. *Cryst. Growth Des.* **2008**, *8*, 3504.

(12) (a) Lai, C. S.; Tiekink, E. R. T. *CrystEngComm* **2004**, *6*, 593. (b) Aromi, G.; Gamez, P.; Roubeau, O.; Berzal, P. C.; Kooijman, H.; Spek, A. L.; Driessen, W. L.; Reedijk, J. *Inorg. Chem.* **2002**, *41*, 3673. (c) Mandon, D.; Machkour, A.; Goetz, S.; Welter, R. *Inorg. Chem.* **2002**, *41*, 5364. (d) Wang, G.-L.; Yang, X.-L.; Zhang, J.; Li, Y.-Z.; Du, H.-B.; You, X.-Z. *Inorg. Chem. Commun.* **2008**, *11*, 1430.

(13) (a) Li, S.-L.; Wu, J.-Y.; Tian, Y.-P.; Tao, X.-T.; Jiang, M.-H.; Fun, H.-K. *Chem. Lett.* **2005**, *34*, 1186. (b) Zheng, N.; Zhang, J.; Bu, X.; Feng, P. *Cryst. Growth Des.* **2007**, *7*, 2576. (c) Pleus, R. J.; Waden, H.; Saak, W.; Haase, D.; Pohl, S. *J. Chem. Soc., Dalton Trans.* **1999**, 2601. (d) Segal, B. M.; Hoveyda, H. R.; Holm, R. H. *Inorg. Chem.* **1998**, *37*, 3440. (e) Huang, S. D.; Lai, C. P.; Barnes, C. L. *Angew. Chem., Int. Ed. Engl.* **1997**, *36*, 1854. (f) Ricciardi, G.; Bencini, A.; Belviso, S.; Bavoso, A.; Lelj, F. *J. Chem. Soc., Dalton Trans.* **1998**, 1985.

(14) (a) O'Keeffe, M.; Eddaoudi, M.; Li, H.; Reineke, T.; Yaghi, O. M. *J. Solid State Chem.* **2000**, *152*, 3. (b) Carlucci, L.; Ciani, G.; Proserpio, D. M. In *Making Crystals by Design: Methods, Techniques, Applications*; Braga, D., Grepioni, F., Eds.; WILEY-VCH: Weinheim, Germany, 2007; p 58.

(15) Batten, S. R.; Robson, R. *Angew. Chem., Int. Ed.* **1998**, *37*, 1460.

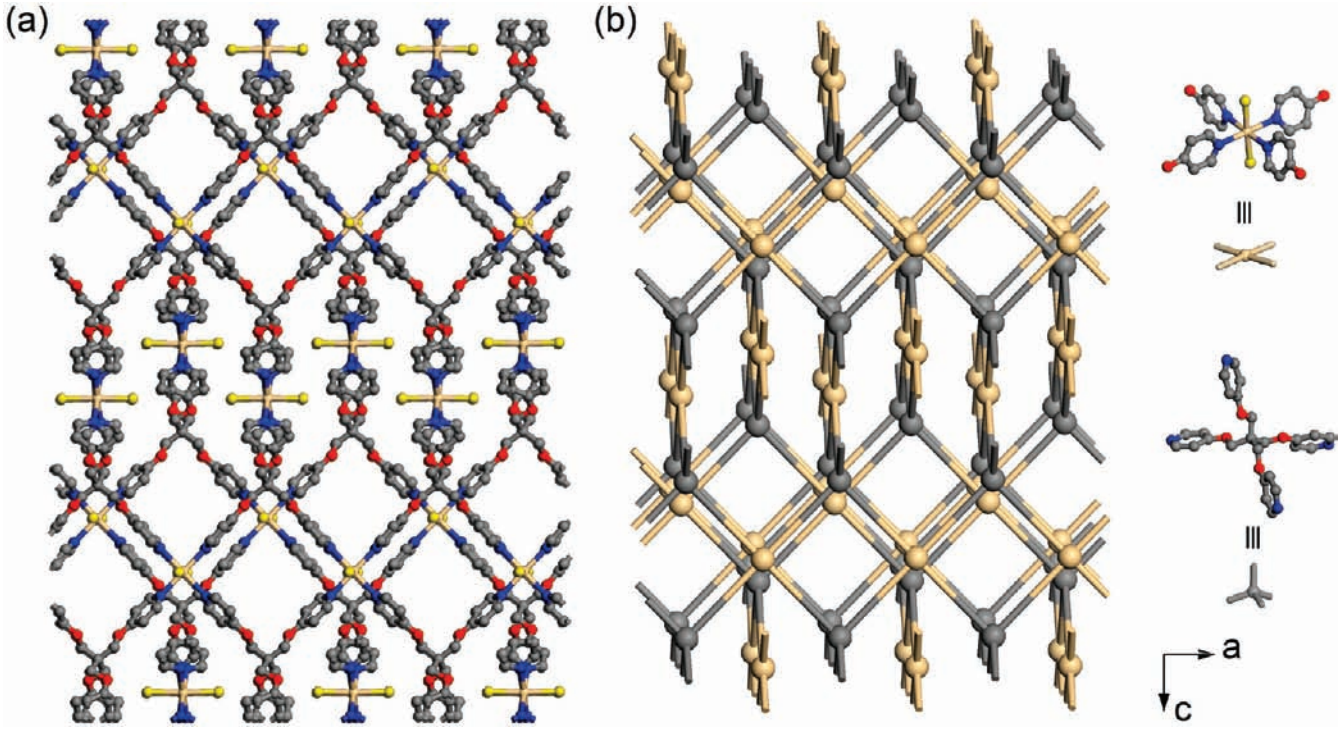

Figure 2. Wire-and-stick (a) and topological (b) representations of 2-fold interpenetrated network of a $4^2 \cdot 8^4$—**pts** net in MSF-*n*. The H atoms and solvent molecules are omitted for clarity. Both MS_2 and tpom are represented as 4-connected nodes.

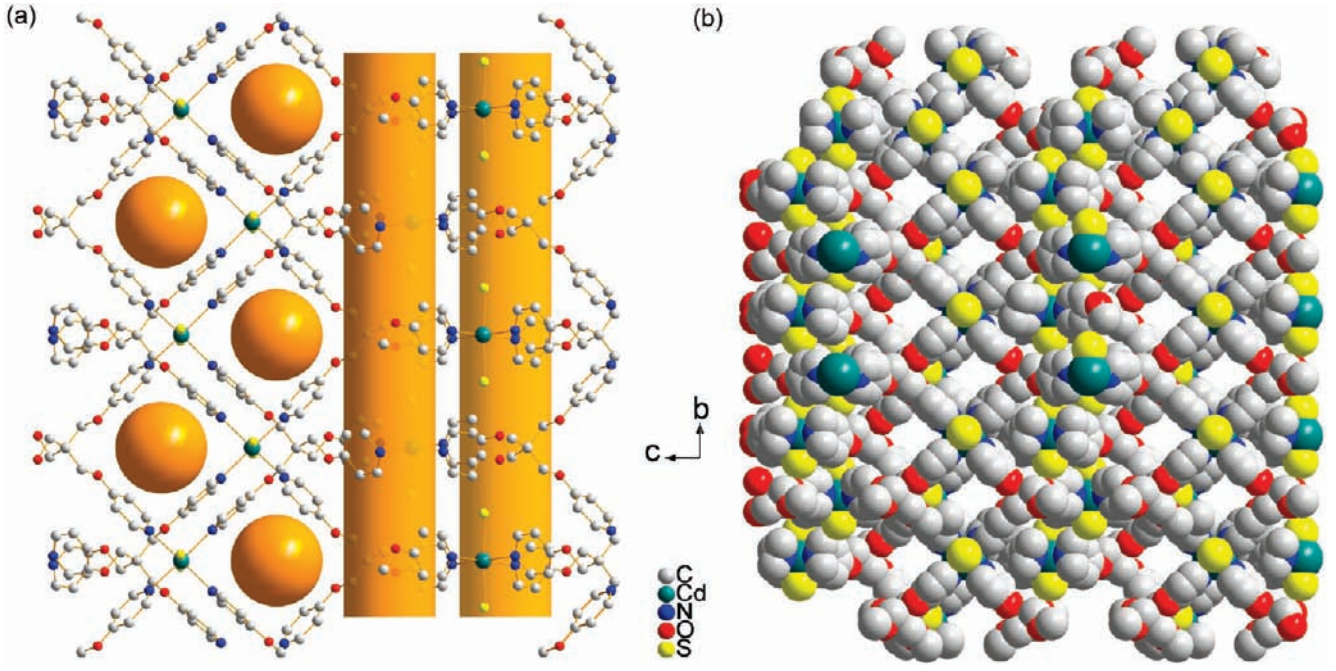

Figure 3. Ball-and-stick (a) and space-filling (b) views of the microporous framework of MSF-*n* along the *a* axis. The H atoms and solvent molecules are omitted for clarity.

There have been several coordination polymers with the tpom ligand reported so far, including 1D chains and 3D frameworks.[16] In these polymers, tpom behaves differently. Tpom is a semirigid tetrapyridyl ligand, in which the four pyridyl groups can flexibly twist around the central quaternary carbon atom to meet different coordination environments. In the chain-like polymer MCOF-10 $[Cd_{17}S_4(SPh)_{26}](tpom)$, tpom acts as a 2-connecting linker, while it is 4-connected in the belt-like MCOF-9 $[Cd_8S(SPh)_{14}]_2(tpom)$ to link two of four corners of the tetrahedral P1 cluster $[Cd_8S(SPh)_{16}]^{2-}$.[16a] In $[M_2(tpom)(D\text{-}cam)_2] \cdot 2H_2O$ (D-H_2cam = D-camphoric

(16) (a) Zhang, Q.; Bu, X.; Lin, Z.; Wu, T.; Feng, P. *Inorg. Chem.* **2008**, *47*, 9724. (b) Liang, L.-L.; Ren, S.-B.; Zhang, J.; Li, Y.-Z.; Du, H.-B.; You, X.-Z. *Cryst. Growth Des.* **2010**, *10*, 1307. (c) Ren, S.-B.; Zhou, L.; Zhang, J.; Zhu, Y.-L.; Li, Y.-Z.; Du, H.-B.; You, X.-Z. *CrystEngComm* **2010**, *12*, 1635. (d) Ren, S.-B.; Zhou, L.; Zhang, J.; Li, Y.-Z.; Du, H.-B.; You, X.-Z. *CrystEngComm* **2009**, *11*, 1834.

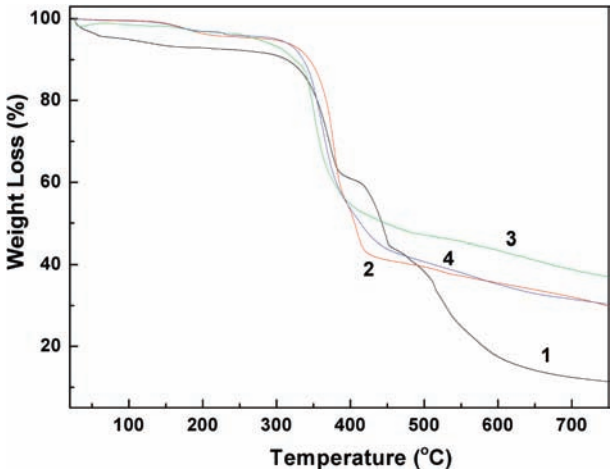

Figure 4. TGA profiles of MSF-*n* (n = 1−4) under nitrogen.

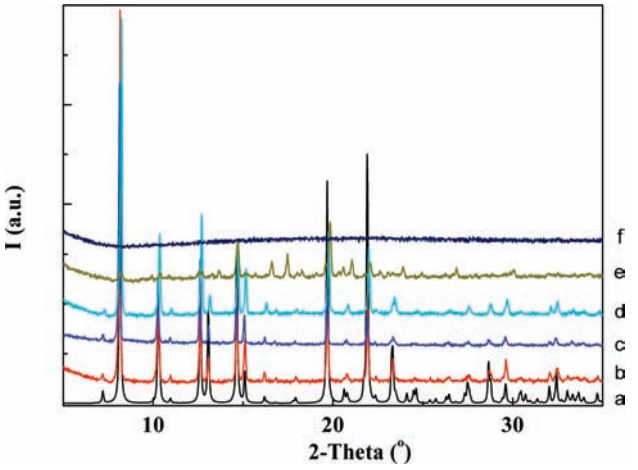

Figure 5. PXRD patterns of MSF-4: (a) simulated; (b) as-synthesized; (c) after gas adsorption measurements; and heated at (d) 150 °C, (e) 250 °C, and (f) 300 °C under N_2 for 2 h each.

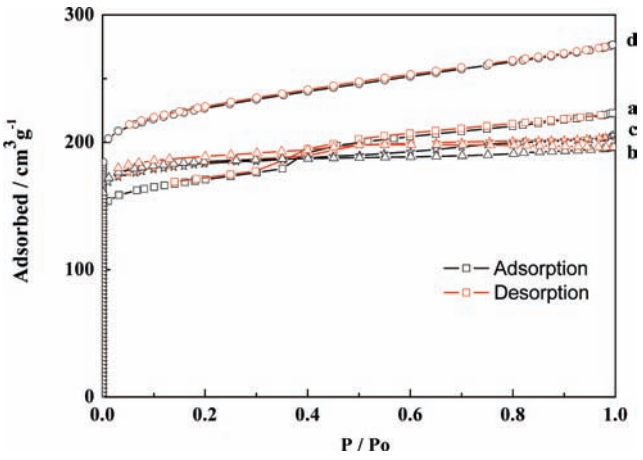

Figure 6. Nitrogen adsorption−desorption isotherms recorded at 77 K for (a) MSF-1, (b) MSF-2, (c) MSF-3, and (d) MSF-4.

acid, M = Zn, Cd)[16b] and $[Zn_2(tpom)(bdc)_2]\cdot 2H_2O$ (bdc = benzene-1,4-dicarboxylic acid),[16c] tetrahedral ligand tpom is severely distorted to a nearly planar geometry, connecting four neighboring M ions to form a 2D sheet, which is then linked by bidentate ligands D-cam and bdc into a 3D quartz and a bimodal 6^28^4 net, respectively. In the triply interpenetrated diamond network $[Cu_4I_4(tpom)]\cdot H_2O$,[16d] tetrahedral tpom is slightly distorted and connected to tetrahedral Cu_4I_4 cubane clusters. MSF-*n*'s are different from the above-mentioned compounds, possessing a binodal PtS network built from a tetrahedral tpom and square planar MS_2 unit. The formation of MSF-*n* shows the rich structural diversity of the ligand tpom in the formation of MOFs.

Thermal Studies. To study the framework stability of MSF-*n* (n = 1−4), thermogravimetric analyses (TGA) and powder X-ray diffraction studies (PXRD) of MSF-*n* samples treated at different temperatures were carried out. TGA was conducted under a flow of nitrogen to determine the thermal stability of MSF-*n*. As shown in Figure 4, MSF-*n* began to lose guest molecules from *ca.* 100 to 310 °C, with weight losses of 10.6, 6.2, 6.4, and 6.2% (calculated 10.4, 6.0, 6.0, 5.9%), for MSF-1, MSF-2, MSF-3, and MSF-4, respectively. Above *ca.* 310 °C, MSF-*n* started to lose its ligands as a result of thermal decomposition. The thermal stabilities of the MSF-*n* frameworks were further checked by X-ray powder diffraction, as exemplified by MSF-4 (Figure 5). The main XRD peaks of MSF-4 heated at 150 °C under N_2 for 2 h match those of the as-synthesized and the simulated ones on the basis of the single crystal structure. The main framework of MSF-4 treated at a higher temperature of 250 °C remained as indicated by the presence of main XRD peaks, but its integrity has been deteriorated as shown by the occurrence of peak broadening and some new peaks. Upon heating at 300 °C for 2 h, the framework of MSF-4 collapsed into an amorphous phase. The results show that MSF-*n* possesses a fairly rigid and robust framework.

Adsorption Properties. Encouraged by thermal studies showing that MSF-*n* is stable upon removal of the guest molecules, we carried out gas adsorption measurements for N_2, H_2, CO_2, and CH_4. As shown in Figure 6, nitrogen adsorption isotherms at 77 K for each compound show type-I behavior with a steep rise in the very low pressure region, suggesting a microporous nature of the four frameworks. The BET surface areas are calculated from N_2 adsorption isotherms to be 575, 622, 617, and 767 m^2/g and Langmuir surface areas of 764, 816, 813, and 1015 m^2/g calculated for MSF-1, MSF-2, MSF-3, and MSF-4, respectively. The solvent-accessible surface area estimated on the basis of the crystal structures of MSF-*n* are 1022, 1081, 1069, and 1027 m^2/g (using a spherical probe of 1.7 Å in diameter), respectively. The discrepancies between the Langmuir surface areas and solvent-accessible surface areas of MSF-1, -2, and -3 indicate the incomplete removal of guest molecules or structural deformation during the thermal activation prior to N_2 adsorption measurements, which are often observed in MOFs.[17] Considering the existence of permanent porosity in MSF-*n* (n = 1−4) and current intense interest in hydrogen storage,[18] we also measured their hydrogen adsorption isotherms at 77 K and low pressure (Figure 7). The hydrogen sorption profiles for MSF-*n* (n = 1−4) also show a type I isotherm curve with a steep uptake in the

(17) Nelson, A. P.; Farha, O. K.; Mulfort, K. L.; Hupp, J. T. *J. Am. Chem. Soc.* **2009**, *131*, 458.

(18) (a) Murray, L. J.; Dinca, M.; Long, J. R. *Chem. Soc. Rev.* **2009**, *38*, 1294. (b) Li, J.-R.; Kuppler, R. J.; Zhou, H.-C. *Chem. Soc. Rev.* **2009**, *38*, 1477. (c) Ma, S.; Zhou, H.-C. *Chem. Commun.* **2010**, *46*, 44.

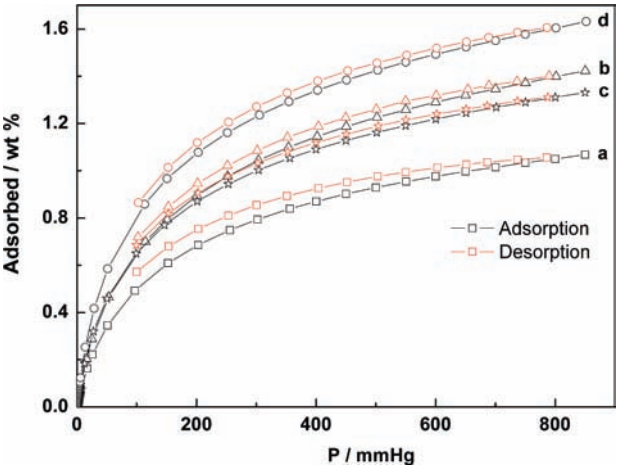

Figure 7. Hydrogen adsorption−desorption isotherms recorded at 77 K for (a) MSF-1, (b) MSF-2, (c) MSF-3, and (d) MSF-4.

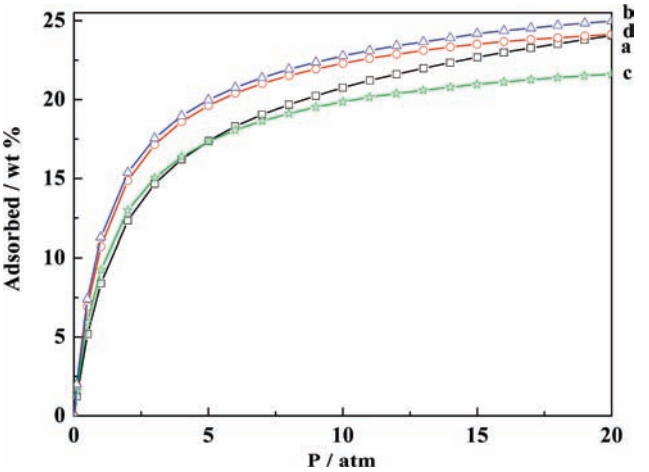

Figure 8. Carbon dioxide adsorption isotherms recorded at room temperature for (a) MSF-1, (b) MSF-2, (c) MSF-3, and (d) MSF-4.

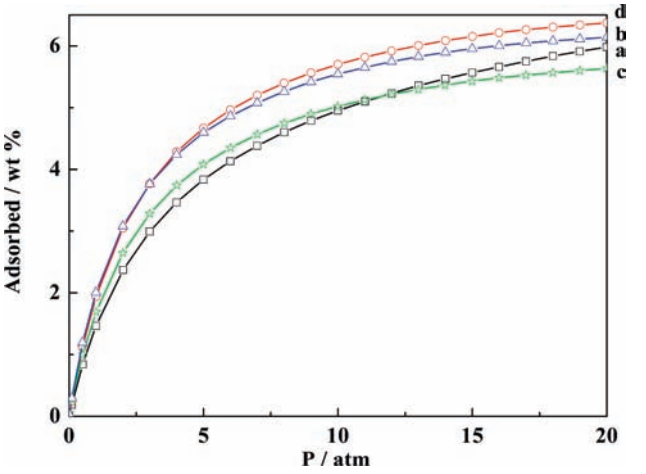

Figure 9. Methane adsorption isotherms recorded at room temperature for (a) MSF-1, (b) MSF-2, (c) MSF-3, and (d) MSF-4.

low-pressure region, indicating a strong affinity of hydrogen molecules toward pore surfaces. The hydrogen adsorption capacities at 77 K and 1 atm are 1.03 wt % (115.8 cm^3/g), 1.37 wt % (153.9 cm^3/g), 1.29 wt % (144.7 cm^3/g), and 1.58 wt % (176.8 cm^3/g) for MSF-1, MSF-2, MSF-3, and MSF-4, respectively, each corresponding to 2.0 H_2 molecules per unit cell. The H_2 adsorption properties of MSF-*n* (n = 1−4) are comparable to many MOFs of moderate H_2 adsorption.[18]

High-pressure gas adsorption measurements were also performed at 293 K to investigate the CH_4 and CO_2 uptake capacities (Figures 8 and 9). At 293 K and 20 atm, MSF-1 adsorbs CO_2 gas up to 24.1 wt % (122.6 cm^3/g STP) and CH_4 up to 6.0 wt % (83.7 cm^3/g STP). MSF-2 adsorbs CO_2 up to 25.0 wt % (127.3 cm^3/g STP) and CH_4 up to 6.1 wt % (85.2 cm^3/g STP). MSF-3 adsorbs CO_2 up to 21.6 wt % (110.0 cm^3/g STP) and CH_4 up to 5.6 wt % (78.2 cm^3/g STP). MSF-4 adsorbs CO_2 up to 24.1 wt % (122.6 cm^3/g STP) and CH_4 up to 6.4 wt % (89.4 cm^3/g STP).

Preliminary experiments show that MSF-*n* also adsorbs organic solvent molecules, as exemplified by MSF-1. The pristine crystals of MSF-1 were soaked in the solvent benzene for about 24 h, then filtered and washed thoroughly with ether, and were then soaked in the solvent $CDCl_3$ for 24 h. ^{1}H NMR (500 MHz, $CDCl_3$) spectra showed the existence of a significant amount of benzene (Figure S4, Supporting Information). Similar experiments showed that MSF-1 can absorb chlorobenzene, *o*-xylene, and *p*-xylene.

Conclusions

We have successfully synthesized four 4,4-connected porous metal organic frameworks, $[M(tpom)S_x(SH)_y]\cdot z(H_2O)$ (MSF-*n*, n = 1, Cd; 2, Mn; 3, Fe; 4, Co; x = 0, y = 2 for 1, 2, and 4 and x = 0.54, y = 1.46 for 3), in the presence of an organic sulfur compound and quadradentate tetrakis(4-pyridyloxymethylene)methane (tpom) ligand. The organic sulfur compound serves as a sulfur source as a result of decomposition under acidic, solvothermal conditions to form coordination polymers of metal hydrosulfides. Four compounds are isostructural and constructed from the semirigid tetrahedral linker and the square planar MS_2 unit, forming a known binodal 4^28^4-**pts** (PtS) net. MSF-*n* (n = 1−4) exhibits permanent porosity confirmed by gas adsorption experiments of H_2, N_2, CO_2, and CH_4.

Acknowledgment. We are grateful for financial support from the National Basic Research Program (2006CB806104 and 2007CB925101), and the National Natural Science Foundation of China (20931004, 50772046 and 20721002).

Supporting Information Available: Figures of the asymmetric unit, Mossbauer spectroscopy, XRPD, ^{1}H NMR, and crystallographic information files (CIF). This material is available free of charge via the Internet at http://pubs.acs.org.